arXiv:1603.00485v2 [cond-mat.str-el] 8 Mar 2016

Tuning a Strain-Induced Orbital Selective Mott Transition in Epitaxial VO_2

Shantanu Mukherjee*,[1] N. F. Quackenbush*,[1] H. Paik,[2] C. Schlueter,[3]
T.-L. Lee,[3] D. G. Schlom,[2,4] L. F. J. Piper,[1,5,*] and Wei-Cheng Lee[1,†]

[1]*Department of Physics, Applied Physics and Astronomy, Binghamton University, Binghamton, New York 13902, USA*
[2]*Department of Materials Science and Engineering, Cornell University, Ithaca, New York 14853-1501, USA*
[3]*Diamond Light Source Ltd., Diamond House, Harwell Science and Innovation Campus, Didcot, Oxfordshire OX11 0DE, UK*
[4]*Kavli Institute at Cornell for Nanoscale Science, Ithaca, New York 14853, USA*
[5]*Materials Science & Engineering, Binghamton University, Binghamton, New York 13902, USA*

(Dated: March 9, 2016)

We present evidence of strain-induced modulation of electron correlation effects and increased orbital anisotropy in the rutile phase of epitaxial VO_2/TiO_2 films from hard x-ray photoelectron spectroscopy and soft V L-edge x-ray absorption spectroscopy, respectively. By using the U(1) slave spin formalism, we further argue that the observed anisotropic correlation effects can be understood by a model of orbital selective Mott transition at a filling that is non-integer, but close to the half-filling. Because the overlaps of wave functions between d orbitals are modified by the strain, orbitally-dependent renormalizations of the bandwidths and the crystal fields occur with the application of strain. These renormalizations generally result in different occupation numbers in different orbitals. We find that if the system has a non-integer filling number near the half-filling such as for VO_2, certain orbitals could reach an occupation number closer to half-filling under the strain, resulting in a strong reduction in the quasiparticle weight Z_α of that orbital. Moreover, an orbital selective Mott transition, defined as the case with $Z_\alpha = 0$ in some, but not all orbitals, could be accessed by epitaxial strain-engineering of correlated electron systems.

*These authors contribute equally.

PACS numbers: 71.10.Hf,71.30.+h,78.70.Dm

Introduction – Mott insulators are characterized by the ratio of U/W, where U refers to the correlation strength and W is the full bandwidth. A Mott state is usually predicted from theoretical models to exist in materials at half filling and when $U/W \sim 1$. However in multi-orbital systems an incipient Mott picture has been proposed with the possibility of an "orbital selective Mott transition" (OSMT). The OSMT scenario was first proposed to understand the physical properties of $Ca_{2-x}Sr_xRuO_4$ by Anisimov[1], stimulating a lot of research efforts on this subject.[2–6] More recently, in the iron based superconductors, OSMT has been suggested to account for the insulating properties driven by the iron vacancy in $K_{1-x}Fe_{2-y}Se_2$. [7–14] In general, the physics of OSMT has relevance to a variety of multi-band materials that are close to a Mott transition, and a better understanding of this phase both theoretically and experimentally would be crucial for advancing our understanding of Mott physics.

Vanadium dioxide (VO_2) is one of the early prototypes for strongly correlated systems near half filling.[15, 16] VO_2 exhibits a metal to insulator transition (MIT) with a concomitant formation of V-V dimers that is generally considered to be driven cooperatively by both Mott and Peierls physics.[16–20] For example, it has been pointed out that the massive orbital switching that occurs upon entering the insulating phase can only be achieved if the system is already close to a Mott insulating regime.[16] A significant theoretical effort has been made to understand this MIT using local density approximation (LDA), LDA + U, LDA + DMFT, etc. [16, 19, 21, 22] Specifically, a Peierls-assisted OSMT mechanism has been proposed to understand the MIT between metallic R and insulating $M1$ phases in bulk VO_2.[22] Furthermore, recent progress in ultra thin epitaxial VO_2 growth using TiO_2 substrates has provided surmounting evidence that electron correlation effects may become enhanced by the large strains, thus pushing the system further into the Mott regime without introducing any dopants.[23–26]. These results suggest that VO_2 is a candidate for exploring the OSMT with epitaxial strain.

In this Letter we present a generalized theory of OSMT to describe how strain can result in quasiparticle weight variation and preferential orbital switching. We perform theoretical calculations to show that an OSMT can be tuned within the metallic phase of VO_2 (R-phase) by applying a strain that enhances the electron correlations. We find that the application of a uniaxial strain tends to make the occupation number on each orbital unequal. As a result, even if the system is slightly away from half filling, the presence of a moderate anisotropic strain along particular directions could render the occupation number in certain orbitals closer to half-filling, leading to an OSMT. Further, by performing hard x-ray photoelectron spectroscopy (HAXPES) and V L-edge x-ray absorption spectroscopy (XAS) on 10 nm epitaxial VO_2 films on

TiO_2(001), (100) and (110), referred to as VO_2(001), VO_2(100), and VO_2(110) (see Supplementary), we show that strain induced electronic effects indeed exist in the metallic phase of VO_2, in an agreement with our theoretical predictions.

Model and Formalism – We have employed the $U(1)$ slave spin formalism[10] on a two orbital model to investigate the effect of strain on the quasiparticle weight near the transition to the featureless Mott phase. The slave spin formalism[6] has been shown to reproduce the Mott transition at the mean-field level in good agreement with DMFT results, and the $U(1)$ version can even obtain the correct non-interacing limit at the mean-field level.[9] We start from a generic two orbital model containing a tight binding Hamiltonian and a multi-orbital Hubbard interaction term representing onsite electron correlations (see Supplementary Materials). Below we briefly summarize the mechanism for studying OSMT in a $U(1)$ slave spin formalism[10] applied to our model Hamiltonian.

Representing the charge degree of freedom by a quantum spin 1/2, the electron creation operator $d^\dagger_{i\alpha\sigma}$ can be written as $d^\dagger_{i\alpha\sigma} = S^+_{i\alpha\sigma} f^\dagger_{i\alpha\sigma}$, where $d^\dagger_{i\alpha\sigma}$ creates an electron on the orbital α with spin σ at site i, $S^+_{i\alpha\sigma}$ is the spin raising operator for the slave spin describing a charge on the orbital α with physical spin σ on the site i, and $f^\dagger_{i\alpha\sigma}$ is the fermionic spinon associated with the physical spin. After solving the mean-field equations subject to the constraints to eliminate the unphysical Hilbert spaces due to the introduction of the slave spins, the quasiparticle weight on orbital α can be obtained by $Z_{\alpha\sigma} \propto |\langle S^+_{\alpha\sigma}\rangle|^2$.[10] Finally, the correlated metallic phase (Mott insulating phase) corresponds to $Z_{\alpha\sigma} \neq 0$ ($Z_{\alpha\sigma} = 0$) for every orbital, and the OSMT is given by $Z_{\alpha\sigma} = 0$ for some orbitals. Note that the OSMT is not a complete insulating state since the quasiparticle weight in certain bands is still finite. We perform the calculations at zero temperature and limit our attention only on the featureless Mott insulating phases. As a result, we have $\langle n_{\alpha\sigma}\rangle = \frac{n_\alpha}{2}$ and $Z_{\alpha\sigma} = Z_\alpha$. In a two orbital model, the half-filling is corresponding to $n = n_1 + n_2 = 2$, and we focus on the case with $1 < n < 2$.

Results – Although the generic tight binding model can describe any two orbital system, we begin by choosing a d_{xz} and d_{yz} two orbital system for the purpose of demonstration (see Supplementary Materials). Now assume that the strain is applied to elongate the system along $\hat{x}$ direction. This strain significantly reduces the wave function overlaps associated with the d_{xz} but has much less effect on the wave function overlaps associated with the d_{yz}. As a result, the bandwidth of d_{xz} orbital should reduce, and we may introduce an effective parameter d such that $t^{11,strain}_{\vec{k}} \equiv (1-d)t^{11}_{\vec{k}}$ Here t^{11} is the hopping matrix element associated with the d_{xz} orbital and $(1-d)$ reflects the bandwidth reduction in the d_{xz} orbital. As a test, we have studied the case with C_4 symmetry and $d = 0$, which is summarized in Supplementary Materials.

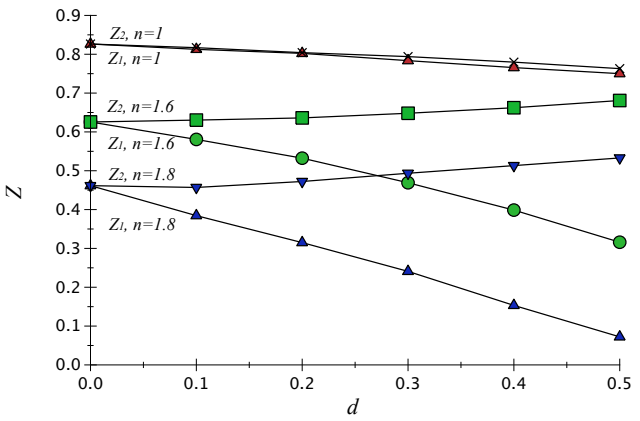

FIG. 1: The orbitally-dependent quasiparticle weight in the case under the strain with $U = 4.5$ for different filling n. At the filling away from the half-filling ($n = 1$), the quasiparticle weights remain almost the same even at large d. In contrast, at the filling near the half-filling ($n = 1.8$ and $n = 1.9$), the quasiparticle weight in d_{xz} (Z_1) reduces significantly as d increases.

Now we turn on the strain by setting $d \neq 0$. There are two effects of d on the d_{xz} orbital. First, since the its bandwidth W_1 is reduced, the ratio of the interaction to the bandwidth U/W_1 increases, leading to stronger correlation effect on d_{xz} orbital. Second, if $n < 2$, the reduction of the bandwidth W_1 tends to attract more electrons to occupy d_{xz} orbital. Therefore we can expect that under the strain, $n_1 = n/2 + x$ and $n_2 = n/2 - x$. This indicates that d_{xz} orbital is pushed even closer to the half-filling and consequently much more correlated. As a result, both effects favor driving d_{xz} more correlated, and an OSMT could be obtained if n is near the half-filling.

The orbitally-dependent quasiparticle weight Z_α as a function of strain with fixed U at different n is presented in Fig. 1. For $n = 1$, the strain does not affect Z_α too much even at quite large d. As n is closer to 2, the difference between Z_1 and Z_2 becomes more prominent, consistent with our discussion above. It should be noted that this result is quite general for a multi-orbital system, and an intriguing point is that one could engineer the OSMT by the strain effect even in a system with non-integer fillings. In the next section, we study the MIT in VO_2 under high strain using the same formalism developed above.

Application to epitaxially strained VO_2 – Although the origin of the MIT in VO_2 is a complicated issue, the dominant bands near the Fermi surface are well-known. The orbital compositions of the three dominant bands near the Fermi surface can be expressed as $|\sigma(d_\parallel)\rangle = |x^2 - y^2\rangle$, and $|\pi_\pm\rangle = \frac{1}{\sqrt{2}}(|xz\rangle \pm |yz\rangle)$. While the leading hopping parameter of σ band mostly comes from the strong direct σ bonding between nearest $V - V$ pairs, the leading

hopping parameters of $\pi_\pm$ bands come from a combination of the direct π bonding between nearest $V-V$ pairs and the second order hoppings via the $V-O$ bonds between $3d$ and $2p$ orbitals.[16, 27] Tanaka estimated[27] $|t^{\sigma\sigma}| \sim |t^{\pi_-\pi_-}| >> |t^{\pi_+\pi_+}|$, which is in close agreement with LDA calculations.[16] Moreover, due to the crystal field effect coming from the oxygen atoms, $\pi_\pm$ bands are pushed to the higher energy, leading to a lower on-site energy in the σ band. As a result, this system can be reasonably approximated as a two-band system with comparable bandwidths in the metallic R phase. A strain on VO_2 due to the (110) or (100)-oriented TiO_2 substrate leads to two important effects that support the OSMT scenario. Firstly, because the c-axis lattice constant of the bulk TiO_2 is longer than that of bulk VO_2 by 3.62%[28], the c-axis is stretched in both VO_2(110) and VO_2(100) (note that the $\hat{x}$-direction in the tetragonal unit cell is along the c-axis[19, 29]). It is found in LDA calculations that a longer c-axis primarily leads to a reduction of the σ orbital hoppings $t^{\sigma\sigma}$ and suppression of the corresponding band width W_σ.[29] Consequently a larger U/W_σ would enhance the electronic correlations in σ band. Secondly, due to the elongation of c-axis, the average $V-O$ bond length would shorten, which enhances the $d-p$ hybridizations, increases the on-site energy of π orbital, and leads to a larger energy difference between the σ and π orbitals. For simplicity, we model the change in the onsite energy as an effective lowering of σ orbital on-site energy. The effects of the strain can then be taken into account by

$$\begin{aligned} t_{\vec{k}}^{\sigma\sigma,strain} &\equiv (1-d)t_{\vec{k}}^{\sigma\sigma} \\ \Delta_\sigma^{strain} &= -(1+Cd)\Delta_\sigma, \end{aligned} \quad (1)$$

where C is a positive constant. It can be seen easily that both effects from the strain strongly favor more occupation numbers in the σ band, thus pushing it closer to half filling.

Moreover, because of the large hybridization between $3d$ orbitals of V and $2p$ orbitals of O, the total occupation number in $3d$ orbitals is in fact in the range of $n = 1.2-2$ instead of 1 as one might expect from a direct counting of the valence charges. Consequently, the OSMT due to the strain effect discussed in the last section is very likely to occur with a moderate d. We adopt the values of $t^{\sigma\sigma}$, $t^{\pi_-\pi_-}$, and the onsite energies derived in Ref. [27] and Eq. 1 to model the strain effect. The quasiparticle weight in the σ band Z_σ at $n = 1.5$ as a function of U and d is plotted in Fig. 2. For small U, Z_σ remains close to 1 and does not depend on d. As U increases, Z_σ develops a significant dependence on d, and an orbital selective Mott transition occurs at a critical $d = d_c$ if U is large enough. Clearly, d_c decreases as U increases, indicating that the OSMT is indeed driven by the strong Coulomb repulsive interaction. Furthermore, we notice that the behavior would be fundamentally different when the c-axis is compressed rather than elongated, as is the case for VO_2(001). This will shorten σ bond distance along the c-direction and would reduce the energy difference between σ and π orbitals, thus keeping their occupations away from half filling in the R phase. As a result, the OSMT would be expected to occur in VO_2(100) and VO_2(110), but not in VO_2(001).

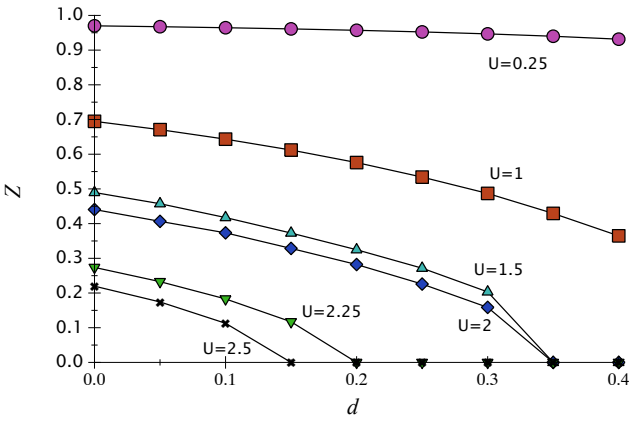

FIG. 2: The quasiparticle weight in the σ band of VO_2 under the strain as a function of U at $n = 1.5$. The hopping parameters for VO_2 are $t^{\sigma\sigma}_{i,i+\hat{x}} = t^{\sigma\sigma}_{i,i+\hat{y}} = -0.25$, $t^{\pi_-\pi_-}_{i,i+\hat{x}} = t^{\pi_-\pi_-}_{i,i+\hat{y}} = 0.22$. The onsite energy due to the crystal field splitting without the strain are $\Delta_\sigma = -0.1$ and $\Delta_\pi = 0.05$. These values are taken from Ref. [27], and the unit of energy is eV. The interband hoppings are small and neglected in Ref. [27], and we set a representative value $t^{\sigma\pi_-}_{i,i+\hat{x}+\hat{y}} = t^{\pi_-\sigma}_{i,i+\hat{x}+\hat{y}} = 0.01$. At large U, an OSMT could occur at small to moderate d.

We emphasize that the increase of the occupation number in the σ band is a direct consequence of the balance between kinetic and interaction energies. Because the bandwidth and the effective onsite energy of the σ band are both lowered by the strain, it is energetically favorable to put more electrons in the σ than in the π_- bands to compromise the interaction energy. While this trend in the occupation numbers can be captured by LDA-based approaches, the significant change in the quasiparticle weight as well as the OSMT found here is attributed to the advantage of the $U(1)$ slave spin formalism. We predict that the occupation number in the σ band could be substantially increased under the strain even in R phase without the dimerization of $V-V$ pairs, and the metallic phase in this region would be a strongly correlated metallic state with vanishing quasiparticle weight in the σ band Z_σ.

To investigate the predicted effect of strain on VO_2 thin films, we have performed HAXPES and polarization dependent XAS of the V L-edge on VO_2(001), VO_2(100), and VO_2(110) in the metallic R phase close to the MIT (see Supplementary). Figure 3a shows the HAXPES of the topmost valence states, while fig. 3b shows the corresponding V L XAS spectra collected from each VO_2 film. All presented spectra are collected at ∼20 °C above

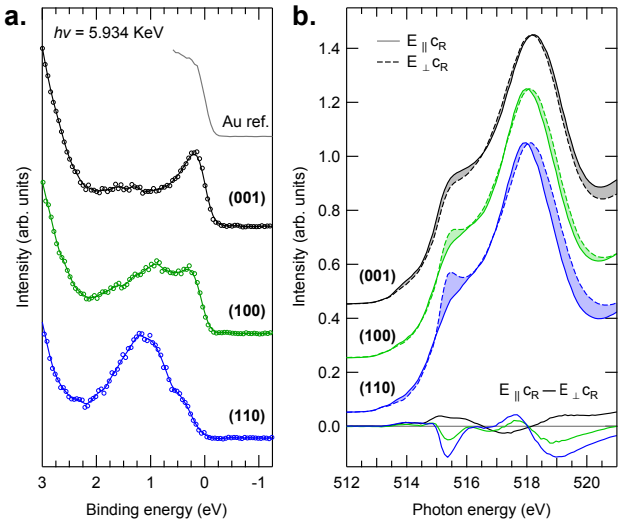

FIG. 3: a. HAXPES of the metallic phases of the three VO_2 strain orientations close to the Fermi level. b. The corresponding polarization dependent V L-edge XAS for the films, along with the orbital dichroism for each case plotted underneath on a common intensity scale.

T_{MIT}, i.e. in the metallic phase. The XAS at the V L-edge were collected with the polarization vector either parallel to the [001] ($E_{\|}c_R$) or [110] ($E_{\perp}c_R$) crystallographic axis. Included at the bottom of fig. 3b are the difference spectra ($E_{\|}c_R$ - $E_{\perp}c_R$) representing the linear orbital dichroism.

Both the valence band HAXPES and weak orbital dichroism of the VO_2(001) closely resemble that of bulk VO_2.[16, 20, 30] In contrast, both the VO_2(100) and (110) films show dramatic deviations from the bulk. The sharp Fermi edge at E_F, indicating Fermi liquid behavior, is weakened in the VO_2(100) case and further so for the (110) case resulting in a more smeared out intensity distribution near the Fermi energy. This behavior is equivalent to the vanishing Z_σ in our model and is typically seen in Mott insulating materials such as in parent cuprate superconductors.[15, 31] Along with these changes at E_F are concurrent increases in orbital anisotropy observed in the V L-edge spectra of the VO_2(100) and VO_2(110) films, indicating preferential filling of certain bands. This demonstrates that the strain, specifically when the c-axis is elongated, can indeed effect both the electron correlations and the orbital occupancy.

The orbital dichroism observed here in the VO_2(100) and VO_2(110) films tends toward that observed for the insulating phase of unstrained VO_2, despite remaining in the metallic phase. Haverkort et al. [16] observed a dramatic switching of the orbital occupancy going from the high temperature rutile to low temperature M1 phase, in which the σ (often referred to as $d_{\|}$) orbital becomes preferentially filled. Our results indicate a similar modification of the orbital occupancy purely induced by strain within the distorted rutile structure. Remarkably, the increased preferential filling of the σ orbital in this case does not require the formation of V–V dimers, supporting our OSMT picture.

Consistent with our OSMT prediction for VO_2, the weak orbital dichroism and the sharp Fermi edge for VO_2(001), when the c-axis is contracted, resemble that of the bulk. Furthermore, we observe that while both VO_2(110) and VO_2(100) have the same stretched c-axis, VO_2(110) exhibits larger orbital dichroism, as well as a weaker Fermi edge, indicating that VO_2(110) is more correlated than VO_2(100). This difference can be attributed to the compression along the out-of-plane direction of the film due to the compensation of the biaxial strain, which is ignored in our theory. The compression in VO_2(110) is along rutile (110) direction (the $\hat{y}$-direction in the unit cell)[19, 29], thus directly effecting the V-O bond lengths. This serves to increase the on-site energy of π orbital due to the enhanced $d-p$ hybridization, which leads to a larger energy difference between the σ and π orbitals. However, in VO_2(100) the compression decreases the distance between V atoms along the rutile a-axis (the $(\hat{y}-\hat{z})$ direction in the unit cell)[19, 29], having a less direct effect on the V-O bond lengths. As a result, the strain effects distinguishing σ and π orbitals are expected to be stronger in VO_2(110). More rigorous theoretical efforts are required to obtain a quantitative description in this aspect.

Conclusion – To summarize, we have studied the effect of strain on multiorbital systems. Because the spatial profile of the orbital wave function are anisotropic, the strain-induced bandwidth reduction and the onsite energy due to the crystal field effect become orbitally-dependent. Based on the $U(1)$ slave spin formalism on a generic two orbital Hubbard model, we have demonstrated that if the system has a total filling which is non-integer, but close to the half-filling, an orbital selective Mott transition could be engineered by the application of strain if the system has strong Coulomb repulsive interactions. By applying this theory to study the highly strained VO_2 in combination with experimental results from spectroscopic studies, we have proposed that an orbital selective Mott state exists in the high temperature phase of coherently strained VO_2 with an elongated c-axis. This state could appear before the M_2 phase emerges, which explains why the region of M_2 phase found in experiments is much narrower than the prediction of Landau-Ginzburg theory.[25]. Our results indicate that Mott physics is crucial to understand the properties of VO_2.

Acknowledgement – We thank Dr. D. O. Scanlon for assisting with the experiments. S. M. and W.-C. L. acknowledge support from a start up fund from Binghamton University. L. F. J. P. and N. F. Q. acknowledge support from the National Science Foundation under DMR 1409912. The work of H.P. and D.G.S. was supported

in part by the Center for Low Energy Systems Technology (LEAST), one of the six SRC STARnet Centers, sponsored by MARCO and DARPA. We thank Diamond Light Source for access to beamline I09 (SI12546) that contributed to the results presented here.

SUPPLEMENTARY MATERIALS

Model

A generic two orbital model can be written as

$$\begin{aligned} H &= H_0 + H_U + H_{pair}, \\ H_0 &= \sum_{\alpha\beta\sigma}\sum_{ij}\left[-t_{ij}^{\alpha\beta} + \delta_{\alpha\beta}\delta_{ij}(\Delta_\alpha - \mu)\right] d^\dagger_{i\alpha\sigma} d_{j\beta\sigma}, \\ H_U &= U\sum_{i\alpha} n_{i\alpha\uparrow}n_{i\alpha\downarrow} + U'\sum_{i,\alpha<\beta,\sigma} n_{i\alpha\sigma}n_{i\beta-\sigma} \\ &+ (U'-J)\sum_{i,\alpha<\beta,\sigma} n_{i\alpha\sigma}n_{i\beta\sigma}, \\ H_{pair} &= -J\sum_i \left[d^\dagger_{i1\uparrow}d_{i1\downarrow}d^\dagger_{i2\downarrow}d_{i2\uparrow} + d^\dagger_{i1\uparrow}d^\dagger_{i1\downarrow}d_{i2\downarrow}d_{i2\uparrow} h.c.\right], \end{aligned} \tag{2}$$

where $d^\dagger_{i\alpha\sigma}$ creates an electron on the orbital α with spin σ at site i, $n_{i\alpha\sigma} = d^\dagger_{i\alpha\sigma}d_{i\alpha\sigma}$, Δ_α is the on-site energy on orbital α due to the crystal field splitting, and $t_{ij}^{\alpha\beta}$ are hopping parameters. $U' = U - 2J$ and $J = 0.2U$ is the Hund's coupling.

The model in Eq. 2 can in principle describe any two orbital systems as long as $\{t_{ij}^{\alpha\beta}\}$ are known. For a d_{xz} and d_{yz} two orbital system H_0 can be written as

$$\begin{aligned} H_0 &= \sum_{\vec{k},\sigma}\sum_{\alpha,\beta=1}^{2}\left[t_{\vec{k}}^{\alpha\beta} + \delta_{\alpha\beta}\delta_{ij}(\Delta_\alpha - \mu)\right] d^\dagger_{\vec{k}\alpha\sigma} d_{\vec{k}\beta\sigma} \\ t_{\vec{k}}^{11} &= -2t_\parallel \cos k_x - 2t_\perp \cos k_y - 4t' \cos k_x \cos k_y, \\ t_{\vec{k}}^{22} &= -2t_\perp \cos k_x - 2t_\parallel \cos k_y - 4t' \cos k_x \cos k_y, \\ t_{\vec{k}}^{21} &= t_{\vec{k}}^{12} = -4t'' \cos k_x \cos k_y, \end{aligned} \tag{3}$$

where $\alpha = 1$ (2) represents the d_{xz} (d_{yz}) orbital, and $t_\parallel$ ($t_\perp$) is the nearest neighbor hoppping via σ (π) bonding respectively.

It is instructive to study the case with C_4 symmetry and $d = 0$. In this case, d_{xz} and d_{yz} orbitals are degenerate, and therefore we have $n_1 = n_2$ and $Z_1 = Z_2 = Z$. Clearly, at n away from the half-filling, Z remains close to 1 even for large U, while at n near the half-filling, Z decreases much more significantly as U increases. Fig. 4 plots Z as a function of U for different values of filling n. The Mott transition occurs around $U/t_\parallel = 4.5$ at exactly $n = 2$.

Experimental Details

Epitaxial VO_2 films were grown on rutile (001), (100), and (110) oriented TiO_2 single crystal substrates by reactive MBE. Substrates were prepared by etching and

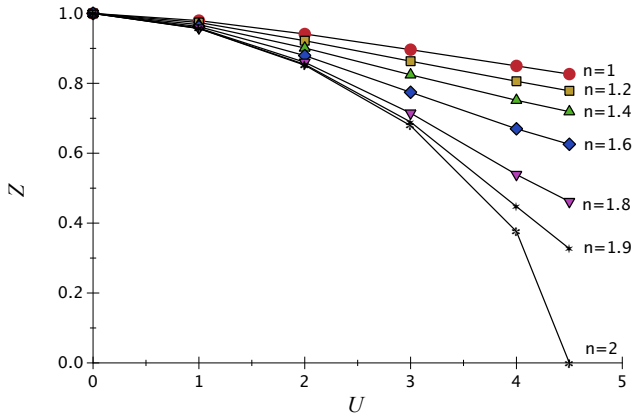

FIG. 4: The quasiparticle weight in the case without the strain as a function of U for different filling n. Because d_{xz} and d_{yz} remain degenerate, $Z_1 = Z_2 = Z$. The parameters in Eq.3 are $t_{\parallel} = 1$, $t_{\perp} = 0.1$, $t' = 0.5$, and $t'' = 0.25$. The Mott transition ($Z = 0$ at $n = 2$) occurs around $U_c = 4.5$ for this choice of hopping parameters.

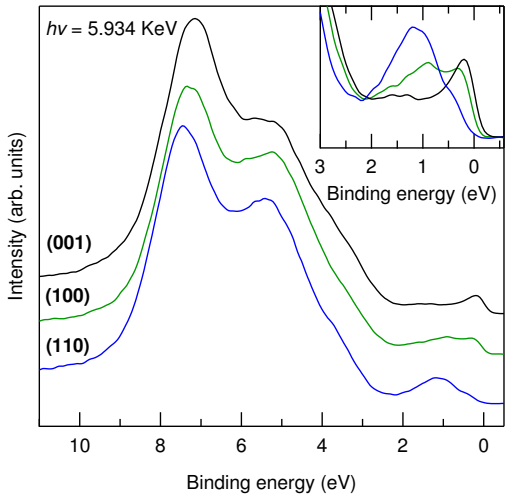

FIG. 5: Full valence band HAXPES of VO_2(001), VO_2(100) and VO_2(110) collected above T_{MIT}.

annealing to have clean and well-defined step and terrace microstructured surfaces. Vanadium and distilled ozone were codeposited onto the substrate held at 250 °C under a distilled ozone background pressure of 1.0×10^{-6} Torr. Following deposition of the desired 10 nm film thickness, the temperature of the sample was rapidly ramped to 350 °C, then immediately cooled to below 100 °C under the same background pressure of distilled ozone to achieve an improved film smoothness and a more abrupt MIT. For further details, the reader is referred to Paik et al. [23].

The HAXPES measurements were performed using a photon energy of hν = 5.934 keV and a pass energy of 200 eV, with a corresponding resolution better than 200

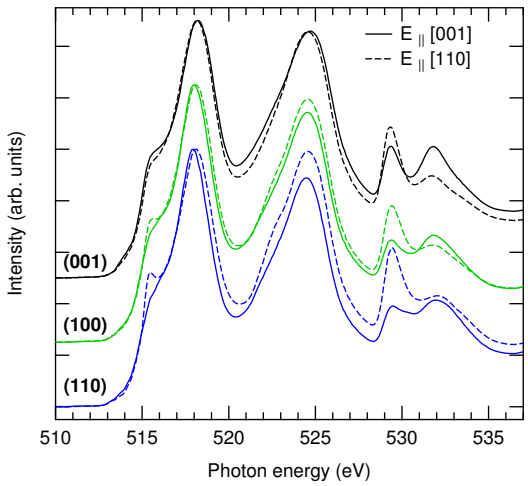

FIG. 6: XAS of the V L-edge (513-528 eV) and O K-edge (528-536 eV) with polarization vector parallel (solid lines) or perpendicular (dashed lines) to the rutile c-axis of VO_2(001), VO_2(100) and VO_2(110) measured above T_{MIT}

meV. The binding energy axes were referenced to both the Au $4f_{7/2}$ and Fermi edge of a Au foil in electrical contact with the film. Figure 5 displays the full valence band spectra of each film presented in the main text. The spectra are normalized to the O 2p states and offset for comparison.

The XAS was performed in total electron yield (TEY) mode by measuring the sample drain current and was normalized by the incoming beam current with a linearly polarized beam. The photon energy axis was calibrated using the Ti $L_{2,3}$ and O K absorption edge features of a rutile TiO_2 single crystal. To achieve the desired alignment between the x-ray polarization and crystallographic direction, the films were rotated in both polar and azimuth. The spectra are normalized to the V L_3 peak to account for the intensity variations due to sample geometry.

The samples were heated with a resistive heating element while monitoring the O K-edge for signatures of the MIT, i.e. V–V dimers. Once the MIT was observed, samples were heated an additional ∼20 °C above T_{MIT} to avoid phase coexistance. Figure 6 shows the polarization dependent XAS for VO_2(001), (100), and (110). The spectra includes both the V L (presented in the main text) and O K-edges. The O K-edge spectra presented here show no evidence V–V dimers, consistent with the rutile metallic phase.

* Electronic address: lpiper@binghamton.edu
† Electronic address: wlee@binghamton.edu

[1] Anisimov, V. I., Nekrasov, I. A., Kondakov, D. E., Rice,

T. M., and Sigrist, M., Eur. Phys. J. B **25**, 191 (2002).
[2] A. Liebsch, Phys. Rev. Lett. **91**, 226401 (2003).
[3] A. Liebsch, Phys. Rev. B **70**, 165103 (2004).
[4] Z. Fang, N. Nagaosa, and K. Terakura, Phys. Rev. B **69**, 045116 (2004).
[5] A. Koga, N. Kawakami, T. M. Rice, and M. Sigrist, Phys. Rev. Lett. **92**, 216402 (2004).
[6] L. de'Medici, A. Georges, and S. Biermann, Phys. Rev. B **72**, 205124 (2005).
[7] L. de' Medici, S. R. Hassan, M. Capone, and X. Dai, Phys. Rev. Lett. **102**, 126401 (2009).
[8] L. de' Medici, Phys. Rev. B **83**, 205112 (2011).
[9] R. Yu and Q. Si, Phys. Rev. B **84**, 235115 (2011).
[10] R. Yu and Q. Si, Phys. Rev. B **86**, 085104 (2012).
[11] M. Yi, D. H. Lu, R. Yu, S. C. Riggs, J.-H. Chu, B. Lv, Z. K. Liu, M. Lu, Y.-T. Cui, M. Hashimoto, et al., Phys. Rev. Lett. **110**, 067003 (2013).
[12] J. Rincón, A. Moreo, G. Alvarez, and E. Dagotto, Phys. Rev. Lett. **112**, 106405 (2014).
[13] L. de' Medici, G. Giovannetti, and M. Capone, Phys. Rev. Lett. **112**, 177001 (2014).
[14] G. Giovannetti, L. de' Medici, M. Aichhorn, and M. Capone, Phys. Rev. B **91**, 085124 (2015).
[15] M. Imada, A. Fujimori, and Y. Tokura, Rev. Mod. Phys. **70**, 1039 (1998).
[16] M. W. Haverkort, Z. Hu, A. Tanaka, W. Reichelt, S. V. Streltsov, M. A. Korotin, V. I. Anisimov, H. H. Hsieh, H.-J. Lin, C. T. Chen, et al., Phys. Rev. Lett. **95**, 196404 (2005).
[17] F. J. Morin, Phys. Rev. Lett. **3**, 34 (1959).
[18] J. B. Goodenough, J. Solid State Chem. **3**, 490 (1971).
[19] V. Eyert, Annalen der Physik **11**, 650 (2002), ISSN 1521-3889.
[20] T. C. Koethe, Z. Hu, M. W. Haverkort, C. Schüßler-Langeheine, F. Venturini, N. B. Brookes, O. Tjernberg, W. Reichelt, H. H. Hsieh, H. J. Lin, et al., Phys. Rev. Lett. **97**, 1 (2006).
[21] S. Biermann, A. Poteryaev, a. I. Lichtenstein, and A. Georges, Phys. Rev. Lett. **94**, 1 (2005), 0410005.
[22] C. Weber, D. D. O'Regan, N. D. M. Hine, M. C. Payne, G. Kotliar, and P. B. Littlewood, Phys. Rev. Lett. **108**, 256402 (2012).
[23] H. Paik, J. a. Moyer, T. Spila, J. W. Tashman, J. a. Mundy, E. Freeman, N. Shukla, J. M. Lapano, R. Engel-Herbert, W. Zander, et al., Appl. Phys. Lett. **107**, 163101 (2015).
[24] N. F. Quackenbush, H. Paik, J. C. Woicik, D. A. Arena, D. G. Schlom, and L. F. J. Piper, Materials **2**, 5452 (2015).
[25] N. F. Quackenbush, H. Paik, M. J. Wahila, S. Sallis, M. E. Holtz, X. Huang, A. Ganose, B. J. Morgan, D. O. Scanlon, Y. Gu, et al., submitted (2016).
[26] J. Laverock, A. R. H. Preston, D. Newby, K. E. Smith, S. Sallis, L. F. J. Piper, S. Kittiwatanakul, J. W. Lu, S. A. Wolf, M. Leandersson, et al., Phys. Rev. B **86**, 195124 (2012).
[27] A. Tanaka, Journal of the Physical Society of Japan **73**, 152 (2004).
[28] Y. Muraoka and Z. Hiroi, Appl. Phys. Lett. **80**, 583 (2002).
[29] B. Lazarovits, K. Kim, K. Haule, and G. Kotliar, Phys. Rev. B **81**, 115117 (2010).
[30] N. F. Quackenbush, J. W. Tashman, J. A. Mundy, S. Sallis, H. Paik, R. Misra, J. A. Moyer, J. H. Guo, D. A. Fischer, J. C. Woicik, et al., Nano letters **13**, 4857 (2013).
[31] Z.-x. Shen, J. W. Allen, J. J. Yeh, J. S. Kang, W. Ellis, W. Spicer, I. Lindau, M. B. Maple, Y. D. Dalichaouch, M. S. Torikachvili, et al., Phys. Rev. B **36**, 8414 (1987).